



ISSN 0975-413X
CODEN (USA): PCHHAX

Der Pharma Chemica, 2016, 8(3):166-179
(<http://derpharmachemica.com/archive.html>)

Experimental and theoretical evaluation of quercetin as a novel and eco-friendly corrosion inhibitor for C38 steel in hydrochloric medium

L. Afia¹, M. Larouj², R. Salghi^{1*}, S. Jodeh^{3*}, M. Zougagh^{4,5}, A. Rasem Hasan⁶
and H. Lgaz^{1,2}

¹Laboratory of Applied Chemistry and Environment, ENSA, Université Ibn Zohr, PO Box 1136, 80000 Agadir, Morocco

²Laboratory separation processes, Faculty of Science, University Ibn Tofail PO Box 242, Kenitra, Morocco

³Department of Chemistry, An-Najah National University, P. O. Box 7, Nablus, Palestine

⁴Regional Institute for Applied Chemistry Research, IRICA, E-13004, Ciudad Real, Spain

⁵Castilla-La Mancha Science and Technology Park, E-02006, Albacete, Spain

⁶Department of Civil Engineering, An-Najah National University, P. O. Box 7, Nablus, Palestine

ABSTRACT

The inhibition performance of quercetin for C38 steel in 1.0M HCl was evaluated by electrochemical measurements: impedance spectroscopy and polarization curves tests. Results obtained reveal that the quercetin acts excellently as a corrosion inhibitor for C38 steel in 1.0 M HCl. The inhibition efficiency increases with the concentration of the inhibitor to reach 98.2 % at 2.10^{-6} M of the quercetin. Polarization curves showed that the quercetin behaves as a mixed-type inhibitor. The adsorption of the inhibitor on the carbon steel surface obeyed the Langmuir adsorption isotherm. The effect of temperature on the corrosion behavior of carbon steel in 1M HCl was also studied. EIS spectra exhibit one capacitive loop and confirm the inhibitive ability. Data obtained from EIS technique, were analyzed to model the corrosion inhibition process through appropriate equivalent circuit model; a constant phase element (CPE) has been used. The activation energy as well as other thermodynamic parameters for the inhibition process was calculated and discussed. Quantum chemical parameters were calculated using *ab initio* and DFT methods to find a good correlation with the inhibition efficiency. A good agreement was found between the theoretical calculations and experimental observations.

Keywords: Corrosion, Steel, Inhibition, Quercetin, HCl solution

INTRODUCTION

Acid solutions are generally used for the removal of undesirable scale and rust in several industrial processes. Hydrochloric and sulphuric acids are widely used in the pickling processes of metals. The use of inhibitors is the most practical methods of protection against corrosion, especially in acidic solutions. Inhibitors are substances which, when added in small concentrations to corrosive media, decrease or prevent the reaction of the metal with the media. The previous researchers show that most organic inhibitors containing hetero atoms such as N, O, P, and S, triple bonds or aromatic rings act as effective inhibitors. Several works have studied the influence of organic compounds on the corrosion of steel in acidic media such asazole [1], pyridine [2] sulfuric [3] and amino acid [4] compounds. But, most of the conventional inhibitors that were developed to combat this endemic problem are highly toxic to human beings and has the potential to degrade the environment. The known hazardous effects of most synthetic organic inhibitors and restrictive environmental regulations have compelled and motivated researchers to focus on the need to develop cheap, non-toxic and environmentally benign natural products as corrosion inhibitors.

Several works have studied the influence of natural organic compounds on the corrosion of steel in acidic media such as: Argan oils and extracts [5], antibacterial drugs [6], linseed oil [7], garlic essential oil [8], and others [9]. The inhibitor

adsorption mode was strictly dependent on the inhibitor structure [10]. Thus, the predominant mechanism of action of an inhibitor may vary with factors such as its concentration, pH, the nature of the anion, the presence of other species in the solution, the extent of reactions to form secondary inhibitors and the nature of the metals [11]. Basically, the adsorption process is constituted of two dependent steps; inhibitor molecules transfer from the bulk aqueous media to the double-layer and then adsorb onto the corroding surface; resulting in construction of a protective layer [12]. Therefore, hydrodynamic flow can be a vital environmental factor which influences on inhibitor performance by facilitating the molecular transport process from bulk solution to surface (positive effect), inducing a surface shear stress and promoting inhibitor desorption (negative effect). Thus, the adsorption of inhibitors may blocks either cathodic, anodic, or both reactions. Flavonoids are widely occurring polyphenols that are found in vegetables, fruits, wine, and tea. They are recognized for their diverse physiological activity, including antioxidation, anticancer, anti-inflammatory, anticarcinogenesis, antidiabetic, antiallergic, acrylamide reduction and anti-vascular smooth muscle contractions [13,]. Flavonoids based on different structures have been identified as flavones, flavanones, flavanols, flavonols, anthocyanidins, and isoflavonoids [14].

Quercetin is a flavonoid found in vegetables, nut, fruits and onion. This compound possesses physiological activity, including the ability to induce glucose uptake in L6 myotubes under oxidative stress [15]. The aims of this paper are to investigate the inhibition effect of quercetin (Scheme 1) on corrosion of C38 steel in 1 M HCl, using electrochemical techniques (potentiodynamic polarisation and impedance measurements) .

MATERIALS AND METHODS

Synthesis of the quercetin

The organic compound 3,3',4',5,7-pentahydroxy-2-phenylchromen-4-one or 2-(3,4-dihydroxyphenyl)-3,5,7-trihydroxy-4H-chromen-4-one obtained from from Sigma company –Aldrich (Germany). Fig. 1 shows the molecular structure of quercetin.

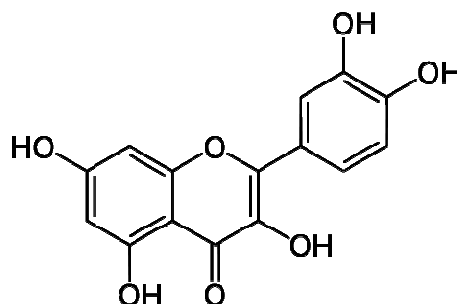


Fig. 1 shows the molecular formula of the investigated inhibitor

Electrochemical tests

The electrochemical study was carried out using a potentiostat PGZ100 piloted by Voltmaster software. This potentiostat is connected to a cell with three electrode thermostats with double wall (Tacussel Standard CEC/TH). A saturated calomel electrode (SCE) and platinum electrode were used as reference and auxiliary electrodes, respectively. The material used for constructing the working electrode was the same used for gravimetric measurements. The surface area exposed to the electrolyte is 0.56 cm². Potentiodynamic polarization curves were plotted at a polarization scan rate of 0.5 mV/s. Before all experiments, the potential was stabilized at free potential during 30 min. The polarisation curves are obtained from -700 mV to -300 mV at 298 K. The solution test is there after de-aerated by bubbling nitrogen. Gas bubbling is maintained prior and through the experiments. In order to investigate the effects of temperature and immersion time on the inhibitor performance, some test were carried out in a temperature range 298–328 K. The electrochemical impedance spectroscopy (EIS) measurements are carried out with the electrochemical system (Tacussel), which included a digital potentiostat model Voltalab PGZ100 computer at E_{corr} after immersion in solution without bubbling. After the determination of steady-state current at a corrosion potential, sine wave voltage (10 mV) peak to peak, at frequencies between 100 kHz and 10 mHz are superimposed on the rest potential. Computer programs automatically controlled the measurements performed at rest potentials after 0.5 hour of exposure at 298 K. The impedance diagrams are given in the Nyquist representation. Experiments are repeated three times to ensure the reproducibility.

Weight loss measurements

Coupons were cut into 2 × 2 × 0.08 cm³ dimensions having composition (0.179% C, 0.165% Si, 0.439% Mn, 0.203% Cu, 0.034% S and Fe balance) are used for weight loss measurements. Prior to all measurements, the exposed area was mechanically abraded with 180, 320, 800 grades of emery papers. The specimens are washed

thoroughly with bidistilled water, degreased and dried with ethanol. Gravimetric measurements are carried out in a double walled glass cell equipped with a thermostated cooling condenser. The solution volume is 80 cm³. The immersion time for the weight loss is 8 h at 298 K.

Solutions preparation

The aggressive solution (1M HCl) was prepared by dilution of analytical grade 37% HCl with double distilled water. The solution tests are freshly prepared before each experiment. Triplicate experiences were made to ensure the reproducibility.

Computational method

The molecular structure of the investigated Quercetin compound was fully and geometrically optimized by using B3LYP Density Functional Theory formalism (DFT) and the 6-31G (d,p) basis set with Gaussian 03 program [16]. The discussion of the theoretical computational studies will be done.

RESULTS AND DISCUSSION

1. Effect of concentration

1.1. Polarization curves

Fig. 2 collects the potentiodynamic polarisation curves of steel in molar HCl in the presence and absence of different concentrations of the quercetin. The corresponding electrochemical parameters values of corrosion current densities (I_{corr}), corrosion potential (E_{corr}), cathodic Tafel slope (β_c) and inhibition efficiency (E_I %) for different concentrations of quercetin are summarised in Table 1.

In this case, the inhibition efficiency is defined as follows:

$$E\% = \left(1 - \frac{I'_{\text{corr}}}{I_{\text{corr}}}\right) \times 100 \quad (1)$$

Where I_{corr} and I'_{corr} are current density in absence and presence of the quercetin respectively. We noted that I_{corr} and I'_{corr} were calculated from the intersection of cathodic and anodic Tafel lines.

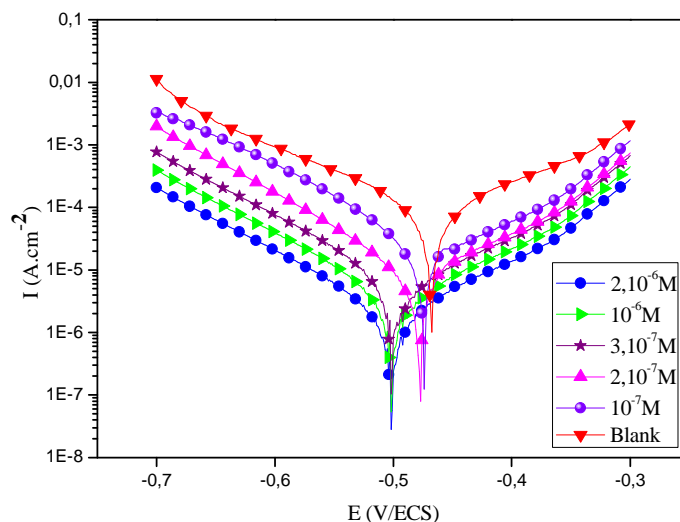


Fig.2 Polarisation curves for steel at various concentrations of quercetin in molar HCl

As it can be seen in Fig. 2, that the presence of quercetin has an inhibitive effect in the both anodic and cathodic parts of the polarization curves. Thus, addition of this inhibitor reduces the carbon steel dissolution as well as retards the hydrogen evolution reaction indicating that the caffeine could be classified as mixed-type inhibitors. However, it seems that in both inhibited systems, the anodic current densities decreases by increasing in inhibitor concentration. It is reported that by increasing the inhibitor concentration, more anodic and cathodic sites will be obstructed [17]. We also remark that the polarization curves are shifted toward more negative potentials and less current density upon addition of the inhibitor. Generally, if the displacement in E_{corr} is >85 mV with respect to E_{corr} in uninhibited solution, the inhibitor can be seen as a cathodic or anodic type [18]. In our study the maximum displacement is 36 mV, which indicates that quercetin acts as a mixed-type inhibitor. In addition, the cathodic current–potential curves

give rise to parallel Tafel lines, which indicate that hydrogen evolution reaction is activation controlled and that the addition of the quercetin does not modify the mechanism of this process [19]. The cathodic Tafel slopes (β_c) are approximately constant suggesting that the inhibiting action occurred by simple blocking of the available cathodic and anodic sites on the metal surface. This shows that the effect of inhibitor on the cathodic reaction is more observable than on the anodic reaction. This result confirms the inhibitive action of the caffeine toward acid corrosion of steel. To conclude, it can be stated that the present inhibitors molecules slow down the corrosion rate by considerably decreasing the active surface area resulted from their adsorption onto the mild steel surface.

Table 1 Electrochemical parameters of C38 steel at various concentrations of quercetin quercetin in 1M HCl and corresponding inhibition efficiency

Concentration (M)	E_{corr} (mV/SCE)	I_{corr} ($\mu\text{A}/\text{cm}^2$)	β_c (mV/dec)	E_I (%)
Blank	-467	114,0	-123	-
10^{-7}	-475	36,5	-107	68,0
$2 \cdot 10^{-7}$	-477	10,0	-98	91,2
$3 \cdot 10^{-7}$	-502	8,0	-104	93,0
10^{-6}	-502	4,3	-99	96,2
$2 \cdot 10^{-6}$	-503	2,1	-101	98,2

Regardless the inhibition mechanism of the above mentioned inhibitor, it can be inferred from Table 1 that even at low concentrations ($2 \cdot 10^{-7}\text{M}$), the compound shows significant efficiency (91.2%). For instance, at $3 \cdot 10^{-7}\text{M}$ concentration reveals 93.0 % efficiency. From the economical point of view, this can be considered as an especial merit for this type of inhibitors. In addition, at the optimum concentration, the highest efficiency of approximately 98% is achieved which is an indication of his superior ability in reduction of mild steel corrosion rate in HCl acidic media.

1.2. Adsorption isotherm

As known, the adsorption isotherms provide important information on interaction between the inhibitor and the metal surface. In this way, Langmuir adsorption isotherm is generally applied because the inhibitors mostly obey this isotherm. Here, an attempt was made to test the Langmuir, Temkin and Frumkin isotherms. The Langmuir adsorption isotherm was found to fit well with the experimental data (Fig. 3), which can be expressed by the equation [20]:

$$\frac{C}{\theta} = \frac{1}{K} + C \quad (2)$$

$$K = \frac{1}{55.5} \exp\left(-\frac{\Delta G_{\text{ads}}}{RT}\right) \quad (3)$$

Where C is the inhibitor concentration, θ the fraction of the surface covered determined by $E/100$, k the equilibrium constant, ΔG_{ads} is the standard free energy of adsorption reaction, R is the universal gas constant, T is the thermodynamic temperature and the value of 55.5 is the concentration of water in the solution in mol/L. Fig. 3 shows the dependence of the ratio C/θ as function of C.

To calculate the surface coverage θ , it was assumed that the inhibition efficiency is due mainly to the blocking effect of the adsorbed species and hence $\theta = IE (\%)/100$.

The plot of C/θ versus C for the quercetin (Fig. 3) yields straight line with correlation coefficient close to 1.0, confirming that the adsorption of this inhibitor is well described by the Langmuir adsorption isotherm. This isotherm based on the assumptions that all the adsorption sites are equivalent and the ability of a molecule to adsorb at a given site is independent of the occupation of nearby sites.

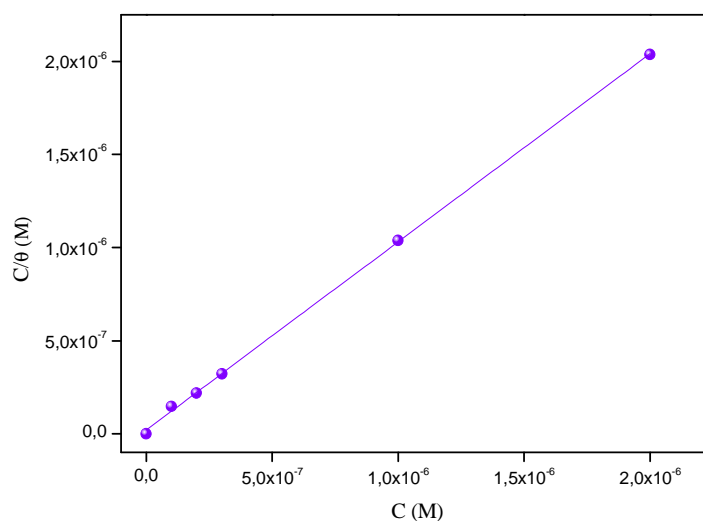


Fig. 3 Plots of Langmuir adsorption isotherm of quercetin on the steel surface at 298K

The ΔG_{ads} value calculated is $-36, 56 \text{ kJ mol}^{-1}$. In general, the values around -40 kJ mol^{-1} or more negative are considered as an indication of charge sharing or charge transferring from an organic specie to the metal surface to form a coordinate type of metallic bond (chemisorption) while those values of approximately -20 kJ mol^{-1} or less negative are assumed for existing electrostatic interactions between inhibitor (physisorption) [21]. Considering ΔG_{ads} value, the adsorption mechanism of quercetin on C38 steel surface in HCl solution probably involves both physisorption and chemisorption however some points are mandatory to be considered. As known, in the solution which includes anions like Cl^- , a competitive adsorption is established between organic inhibitors and anions. In chemisorption type, the protonated inhibitor loses its associated proton when entering the double layer and chemisorbs by donating electrons onto the metal. The inhibitory action may be attributed to the presence O atoms (fig.4) in the linear chain which humbly reinforces the adsorption of the quercetin ring.

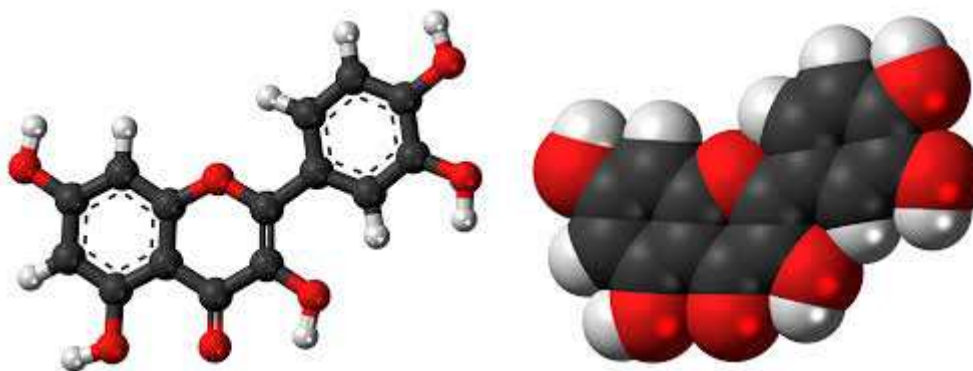


Fig. 4 shows the dimensional and three-dimensional structure of the investigated inhibitor

1.3. Electrochemical impedance spectroscopy measurements

The EIS measurements of the C38 steel were obtained in 1 M HCl solution in the absence and presence of various concentrations of quercetin at 298K and Nyquist plots were presented in Fig. 5.

The EIS results are simulated by the equivalent circuit shown in Fig. 6 to pure electric models that could verify or rule out mechanistic models and enable the calculation of numerical values corresponding to the physical and/or chemical properties of the electrochemical system under investigation [45]. In the electrical equivalent circuit, R_s is the solution resistance, R_T the charge transfer resistance and C_{dl} is the double layer capacitance.

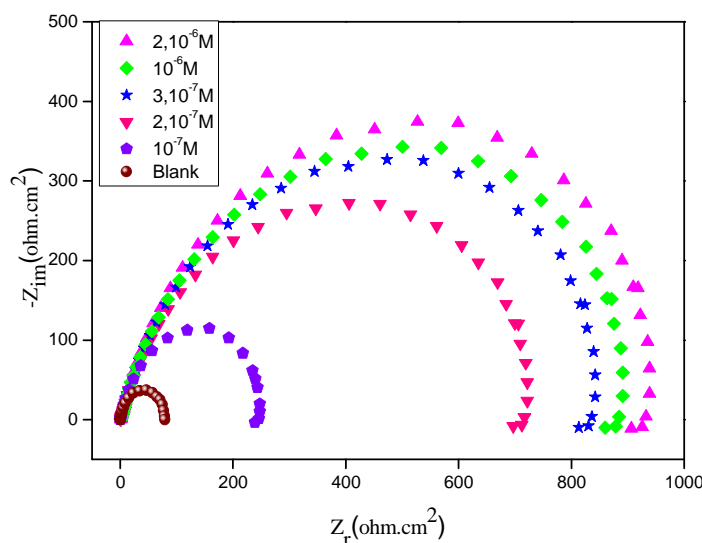


Fig. 5 Nyquist diagrams for C38 steel electrode with and without quercetin at E_{corr}

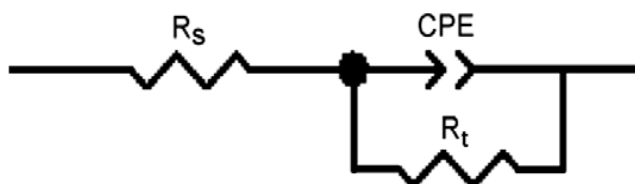


Fig. 6 The electrochemical equivalent circuit used to fit the impedance spectra.

The electrochemical impedance parameters derived from this investigation are mentioned in Table 2. The values of the polarization resistance were calculated by subtracting the high frequency intersection from the low frequency intersection [22].

Double layer capacitance values were obtained at maximum frequency (f_{max}), at which the imaginary component of the Nyquist plot is maximum, and calculated using the following equation:

$$C_{dl} = \frac{1}{2 \cdot \pi \cdot f_{max} \cdot R_t} \quad (4)$$

With C_{dl} : Double layer capacitance ($\mu\text{F} \cdot \text{cm}^{-2}$); f_{max} : maximum frequency (Hz) and R_t : Charge transfer resistance ($\Omega \cdot \text{cm}^2$).

The inhibition efficiency can be calculated by the following formula:

$$E_{Rt} \% = \frac{(R_t - R_t^0)}{R_t} \times 100 \quad (5)$$

Were R_t and R_t^0 are the charge transfer resistances in inhibited and uninhibited solutions respectively.

The impedance spectra for carbon steel in 1M HCl at 298 (Fig. 5) showed one single depressed capacitive loop. The same trend (one capacitive loop) was also noticed for C38 steel immersed in 1M HCl containing quercetin. The shape is maintained throughout the whole concentrations, indicating that almost no change in the corrosion mechanism occurred due to the inhibitor addition [23]. The obtained Nyquist impedance diagrams in most cases does not show perfect semicircle, generally referred to the frequency dispersion of interfacial impedance. This anomalous phenomenon may be attributed to the inhomogeneity of the electrode surface arising from surface roughness or interfacial phenomena [24]. When a non-ideal frequency response is present, it is commonly accepted to employ distributed circuit elements in an equivalent circuit. The most widely used is the constant phase element (CPE), which has a non-integer power dependence on the frequency [25]. Often a CPE is used in a model in place of a capacitor to compensate for non-homogeneity in the system. The impedance of a CPE is described by the expression:

$$Z_{CPE} = Y^{-1} (j\omega)^{-n} \quad (6)$$

Where CPE is a constant phase element, Y is the magnitude of CPE, ω is the angular frequency ($2\pi f_{\max}$), and the deviation parameter n is a valuable criterion of the nature of the metal surface and reflects microscopic fluctuations of the surface. For $n = 0$, Z_{CPE} represents resistance with $R = Y^{-1}$; $n = -1$ an inductance with $L = Y^{-1}$, $n = 1$ an ideal capacitor with $C = Y$.

The idealized capacitance (C_{id}) values can be described by CPE parameter values Y and n using the following expression:

$$C_{id} = Y\omega^{n-1} / \sin(n\pi/2) \quad (7)$$

Fig. 4 shows the electrical equivalent circuit employed to analyze the impedance spectra with one capacitive loop. As an example, the Nyquist plots in 1M HCl solution in the absence and presence of 2.10^{-7} M of quercetin are presented in Fig. 5 and 6 respectively.

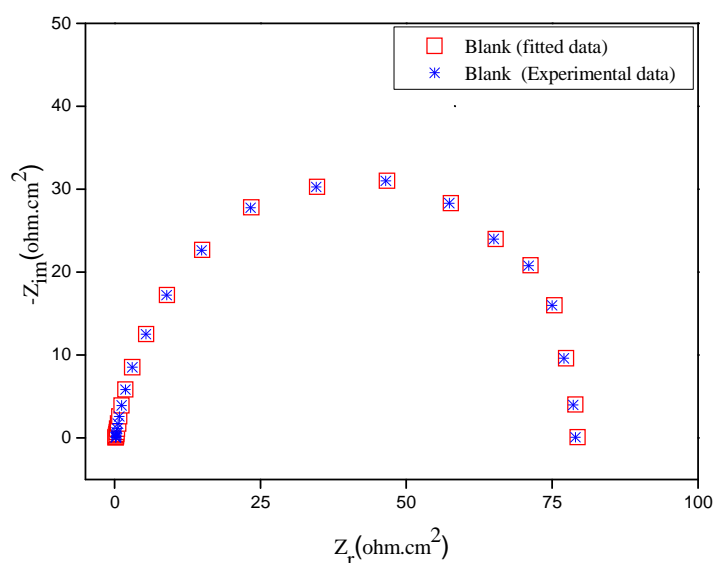


Fig. 5. EIS Nyquist plots for mild steel in 1M HCl

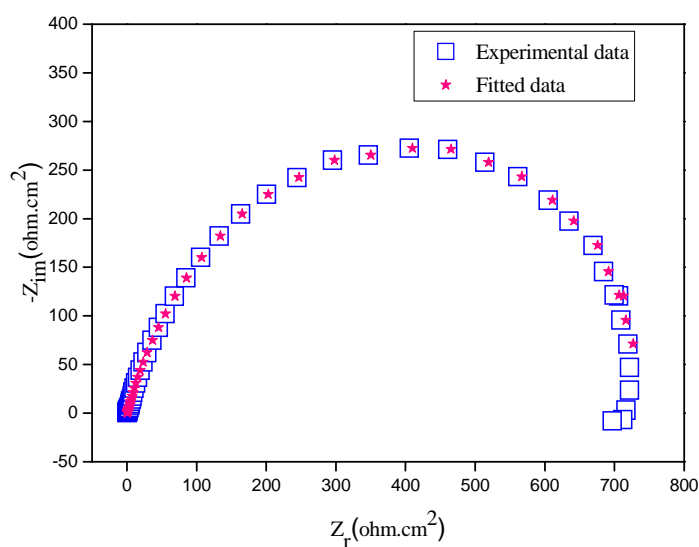


Fig. 6. EIS Nyquist plots for mild steel in 1M HCl + 2.10^{-7} M of quercetin interface

Excellent fit with this model was obtained with our experimental data (Figs. 3). It is observed that the fitted data match the experimental, with an average error of about 0.01%. R_t values were simultaneously determined by analysis of the complex-plane impedance plots and the equivalent circuit model and the result are very similar with insignificant changes.

Table 2 Electrochemical Impedance parameters for corrosion of steel in acid medium at various contents of quercetin

Concentration (M)	R_t ($\Omega \cdot \text{cm}^2$)	$10^{-5} A$ ($\Omega^{-1} S^n \text{ cm}^2$)	n	f_{max} (Hz)	C_{dl} ($\mu\text{F}/\text{cm}^2$)	E_{RT} (%)
Blank	74	12,82	0,8984	79	75,72	-
10^{-7}	247	5,97	0,8869	51	34,87	70,0
$2 \cdot 10^{-7}$	720	5,24	0,8724	29	32,45	89,7
$3 \cdot 10^{-7}$	839	4,38	0,8698	19	26,71	91,2
10^{-6}	890	2,76	0,8475	14	14,17	91,7
$2 \cdot 10^{-6}$	935	2,23	0,8259	11	9,86	92,1

As seen from the impedance data given in Table 2, that introduction of the quercetin into the acid solution caused the charge transfer resistance to increase, while reducing the double-layer capacitance and consequently the inhibition efficiency increases to reach 92.1% at $2 \cdot 10^{-6} \text{M}$ as concentration. An increase in R_t refers to more impediment of the active area at the metal surface as a result of the increase in inhibitor concentration. Mainly, the decrease in C_{dl} value is attributed to the replacement of the adsorbed water molecules at the metal surface by the inhibitor molecules having lower dielectric constant. Also, the decrease in surface area which acts as a site for charging may be considered as another reason for the C_{dl} decrease [26]. These points suggest that the role of inhibitor molecules is preceded by the adsorption at the metal-solution interface. We also remark the decrease in n values of the inhibited system in comparison with 1 M HCl blank solution. Generally, the deviation of n from the values of 1 can be considered as a measure of the surface inhomogeneity [27]. The results obtained from the electrochemical techniques in acidic solution were in good agreement with an insignificant variation.

2. Effect of temperature

1.2 Polarization curves

Temperature can modify the interaction between the carbon steel electrode and the acidic medium in the absence and the presence of inhibitors. For this purpose, we made potentiostatic polarization in the range of temperature 298 to 328 K, in the absence and presence of quercetin at 10^{-6}M . The corresponding data are shown in fig 8, 9 and Table 4.

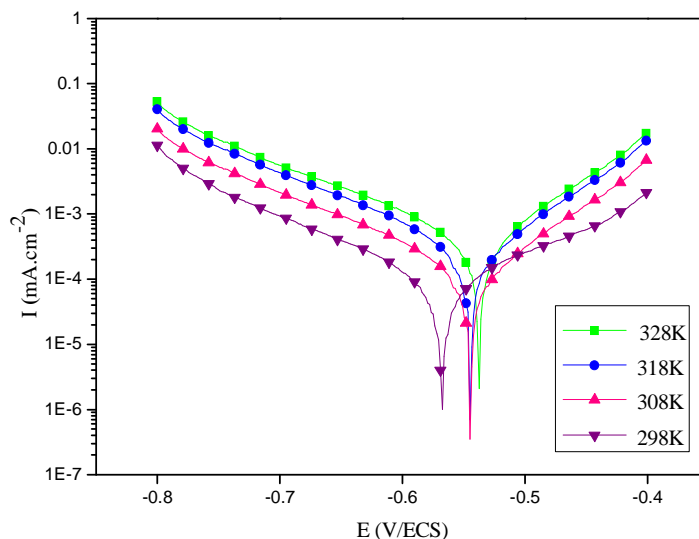


Fig. 8. Polarisation curves of C38 steel in 1M HCl

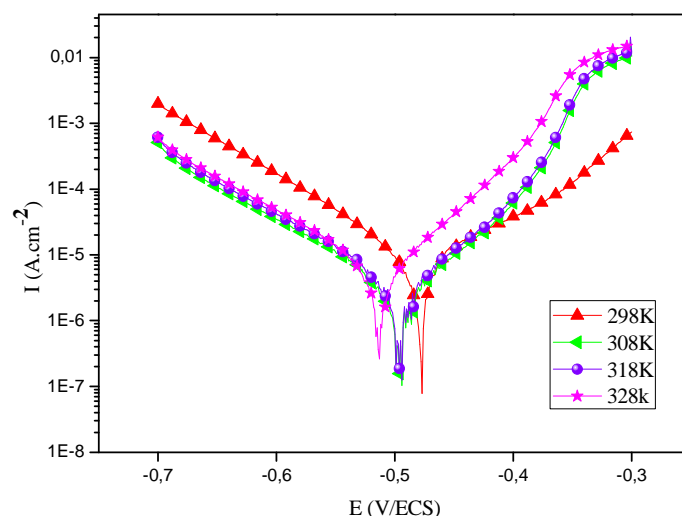


Fig. 9. Polarisation curves of C38 steel in 1M HCl in the presence of 10^{-6} M of quercetin at different temperatures

Table 4. Effect of temperature on the steel corrosion in the absence and presence of quercetin at different concentrations

Inhibitor	Temperature	E_{corr} (mV/SCE)	I_{corr} ($\mu\text{A}/\text{cm}^2$)	$-b_c$ (mV/dec)	E_I (%)
Blank	298	-567	114,0	123	-
	308	-544	157	126	-
	318	-545	305	129	-
	328	-537	399	136	-
quercetin 10^{-6} M	298	-477	10,0	98	96,2
	308	-496	3	101	98,1
	318	-496	4	102	98,7
	328	-513	6	102	98,5

As seen from Fig.8, 9 and Table 3 the value of corrosion current density increases in uninhibited solution and decrease slightly in inhibited medium. The value of inhibition efficiency increases slightly with the increase in the temperature. Thus, quercetin acts as a temperature-independent inhibitor. The nearly constant efficiency of the inhibitor in the temperature range studied can be considered as the slight change in the nature of the adsorption mode: physisorption of the inhibitor is dominant in the temperature range studied, while chemisorption accompanied by physisorption can occur slightly with increasing the temperature.

2.2 Kinetic parameters

In order to obtain more details on the corrosion process, activation kinetic parameters such as activation energies in free and inhibited acid were calculated using Arrhenius equation:

$$I_{corr} = A \exp\left(-\frac{E_a}{RT}\right) \quad (8)$$

Where A is Arrhenius factor, E_a is the apparent activation corrosion energy, R is the perfect gas constant and T the absolute temperature.

Plotting ($\log I_{corr}$) versus $1/T$ gives straight lines as revealed from Fig.10.

The activation energy values obtained are 13.54 and 35.92 kJ/mol for 10^{-6} M of quercetin and free acid, respectively. Notably, the energy barrier of the corrosion reaction in the inhibited medium is lower than that obtained in the free solution. The lower value of the activation energy of the corrosion process in the presence of inhibitor compared to that in its absence is attributed to the existence of chemical process in the adsorption of inhibitor on steel surface. The decrease of E_a value can be interpreted as slow rate of inhibitor adsorption with a resultant closer approach to equilibrium during the experiments at high temperature. Behpour et al. [28] explained the change of the activation energy from energetic heterogeneity of the surface as follows. Assuming that energetic surface is heterogeneous, active centers of the surface have different energy. Two possibilities may exist: in the first case, the inhibitor is

adsorbed on the most active adsorption sites (having the lowest energy) and the corrosion process takes place predominantly on the active sites of higher energy, which results in the higher activation energy. In the second case, a smaller number of more active sites remain uncovered which take part in the corrosion process, resulting in the lower activation energy. However, Vrac̆ar and Draz̆ic [29] argued that the criteria, adsorption type obtained from the change of activation energy, cannot be taken as decisive due to competitive adsorption with water whose removal from the surface requires also some activation energy. On the other words, the so-called chemisorption process may contain physical process simultaneously and vice versa.

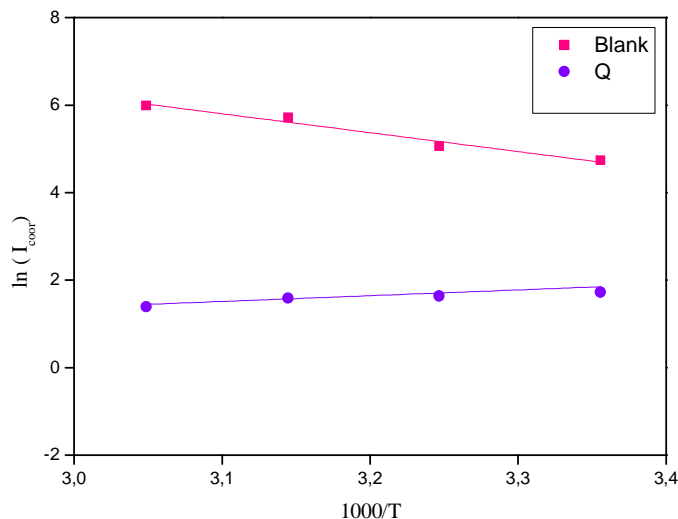


Fig.10 Arrhenius plots of steel in 1 M HCl with and without 10^{-6} M of quercetin

Kinetic parameters, such as enthalpy and entropy of corrosion process, may be evaluated from the effect of temperature. An alternative formulation of Arrhenius equation is (9):

$$I_{corr} = \frac{RT}{Nh} \cdot \exp\left(\frac{\Delta S^*}{R}\right) \cdot \exp\left(-\frac{\Delta H^*}{RT}\right) \quad (9)$$

Where N is the Avogadro's number, h the Plank's constant, R is the perfect gas constant, ΔS^* and ΔH^* the entropy and enthalpy of activation, respectively.

Fig. 11 shows a plot of $\ln(W/T)$ against $1/T$ for quercetin. Straight lines are obtained with a slope of $(-\Delta H^*/R)$ and an intercept of $(\ln R/Nh + \Delta S^*/R)$ from which the values of ΔH^* and ΔS^* are calculated respectively (Table 5).

The value of free energy ΔG^* is deduced from the formula (10):

$$\Delta G^* = \Delta H^* - T\Delta S^* \quad (10)$$

Table. 5 The values of activation parameters ΔH^* , ΔS^* and ΔG^* for mild steel in 1M HCl in the absence and the presence of 10^{-6} M of quercetin

Inhibitor	ΔH^* (kJ/mole)	ΔS^* (J/mole ⁻¹ .k ⁻¹)	ΔG^* (kJ/mole à T=298K)	Ea- ΔH^*
Blank	33,33	-184,98	55,16	2,60
Quercetin (10^{-6} M)	16,15	-288,14	102,01	2,60

The values of E_a and ΔH^* are close to each other as expected from the concept of transition state theory and vary in the same manner on the addition of inhibitor. The positive sign of ΔH^* has been attributed to the endothermic nature of the C38 steel dissolution process. The higher values of ΔS^* for inhibited solutions can be attributed to the increase in solvent entropy. However, C38 steel corrosion in the free acid was characterized by the more negative ΔS^* value which implies that the activation complex in the rate determining step required association rather than dissociation [30]. The ΔG^* value for inhibited systems were more positive than that for the uninhibited systems

revealing that in presence of inhibitor, the activated corrosion complex becomes less stable as compared to its absence.

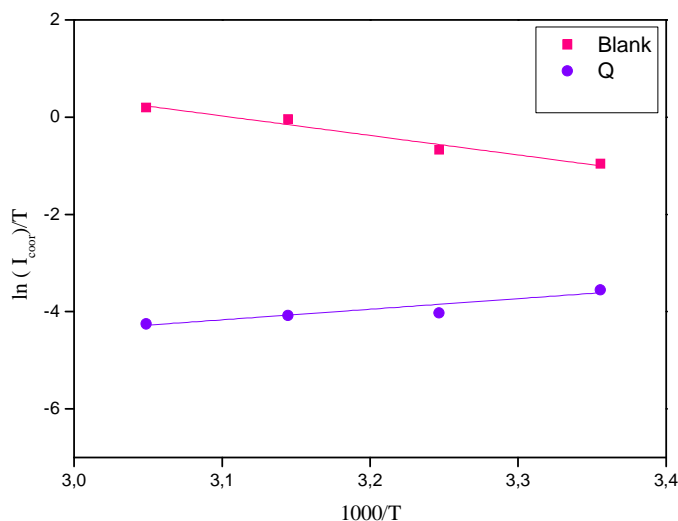


Fig.11. Relation between $\ln(W_{\text{corr}}/T)$ and $1000/T$ in acid at different temperatures

3. Quantum chemical study

The following quantum chemical indices were considered to research the relationship of molecular structure and inhibition effect: the energy of the highest occupied molecular orbital (E_{HOMO}), the energy of the lowest unoccupied molecular orbital (E_{LUMO}), energy band gap $\Delta E = E_{\text{HOMO}} - E_{\text{LUMO}}$, the dipole moment (μ), chemical hardness (η), electronic chemical potential (π), softness (σ), susceptibility (χ) and the number of electrons transferred (ΔN).

The concepts of these parameters are related to each other as follows:

$$\pi = -\chi \quad (11)$$

$$\pi = \frac{E_{\text{HOMO}} + E_{\text{LUMO}}}{2} \quad (12)$$

$$\eta = \frac{E_{\text{HOMO}} - E_{\text{LUMO}}}{2} \quad (13)$$

$$\Delta E = E_{\text{HOMO}} - E_{\text{LUMO}} \quad (14)$$

$$\sigma = \frac{1}{\eta} \quad (15)$$

$$\Delta N = \frac{\chi_{\text{Fe}} - \chi_{\text{inh}}}{2(\eta_{\text{Fe}} + \eta_{\text{inh}})} \quad (16)$$

According to frontier molecular orbital theory, the chemical reactivity is a function of interaction between HOMO and LUMO levels of reacting species. Theoretical calculations were conducted in order to provide molecular-level understanding of the corrosion inhibition behavior of quercetin inhibitor. Fig. 12 and Fig 13 show the optimized structure, HOMO and LUMO orbitals of quercetin compound. The quantum chemical parameters were calculated and listed in Table 6. These parameters were found to be extremely important properties for interpreting the chemical reactivity of inhibitors with metal surfaces [31].

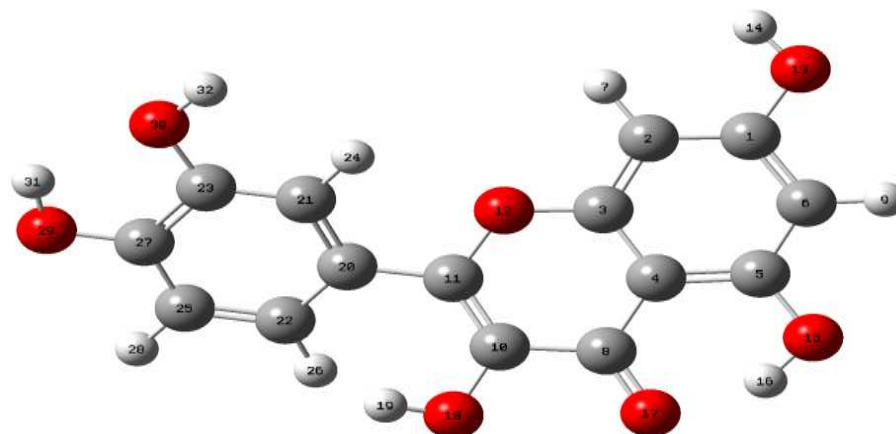


Fig. 12 Optimized structure of quercetin

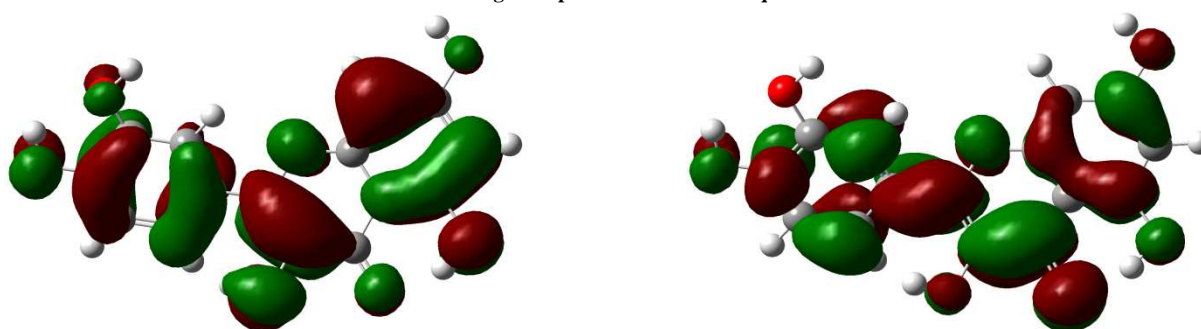


Fig.13 Frontier molecule orbital density distributions of the synthesized inhibitor

Table 6. Quantum chemical parameters for quercetin

Molecule	E_{HOMO} (eV)	E_{LUMO} (eV)	ΔE (eV)	μ (eV)	TE(eV)	η (eV)	σ (eV ⁻¹)	χ (eV)	ΔN	IE (%)
Quercetin	-5.6736	-1.6917	3.9813	7.9103	-30046	-1.9907	0.5023	3.6827	0.833	92.1

Analysis of Fig. 13 shows that the distribution of two energies HOMO and LUMO, we can see that the electron density of the HOMO and LUMO location was distributed almost of the entire molecule. E_{HOMO} indicates a tendency of the molecule to donate electrons to an acceptor molecule while E_{LUMO} represents the ability of the molecule to accept electrons. High values of $E_{\text{HOMO}} = -5.6736\text{eV}$ show a higher propensity of a molecule to donate electrons whereas low value of $E_{\text{LUMO}} = -1.6917\text{eV}$ suggests the ease to which the molecule can accept electrons. In other words, the inhibition efficiency increases if the compound can donate electrons from its HOMO to the LUMO of the metal, whereby chelation on the metal surface occurs. The energy gap, ΔE , is an important parameter which indicates the reactivity tendency of a molecule toward the metal surface. As ΔE decreases, the reactivity of the molecule increases leading to an increase in adsorption onto a metal surface. A molecule with low energy gap is more polarizable and is generally associated with high chemical reactivity and low kinetic stability. The ΔE explained that, the greater inhibition effect could be related to the lower energy difference, i.e. to the quercetin molecules that could be more readily excited and undergo a charge transfer interaction with the metal surface. As can be seen in Table 6, the E_{HOMO} , E_{LUMO} and ΔE show that, quercetin good corrosion inhibitor for carbon steel corrosion in 1.0 M HCl. The dipole moment (μ in Debye) is another important electronic parameter that results from non uniform distribution of charges on the various atoms in the molecule. The high value of dipole moment probably increases the adsorption between chemical compound and metal surface [32]. In our study the value 4.8131 (Debye) of quercetin enumerates its better inhibition efficiency. The number of electrons transferred (ΔN) was also calculated and tabulated in Table 6. Values of ΔN show that the inhibition efficiency resulting from electron donation agrees with Lukovits's study. If $\Delta N < 3.6$, the inhibition efficiency increases by increasing electron-donating ability of these inhibitors to donate electrons to the metal surface. The results indicate that ΔN values correlates strongly with experimental inhibition efficiencies. Molecular electrostatic potential (MEP) is related to the electronic density and a very useful descriptor for determining active sites for electrophilic attacks and nucleophilic attack. The MEP of non-protonated inhibitors were given in Fig. 14. To investigate reactive sites for electrophilic and nucleophilic attack, the regions of the MEP for the quercetin, is composed by DFT calculation using the optimized geometry at the B3LYP/6-3G (d,p). As visual in Fig. 14, red and yellow colors indicated for the negative

regions of the MEP are related to electrophilic reactivity, while blue colors indicated for positive regions to nucleophilic reactivity. As can be seen from Fig. 14, quercetin has two possible sites (O15 and O17 atoms) for electrophilic attack. According to these calculated results, the regions of MEP show that the negative potential sites are on electronegative atoms (oxygen atoms) as well as the positive potential sites are around the hydrogen atoms.

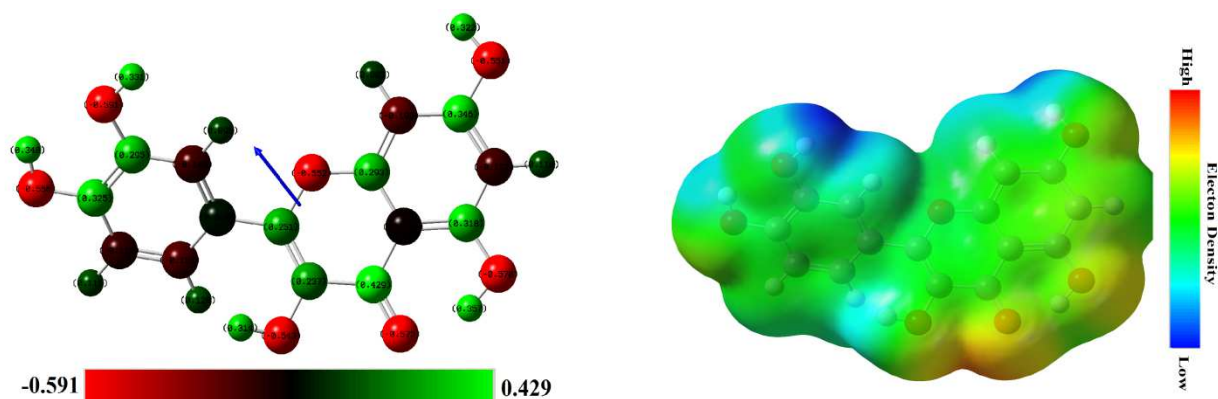


Fig.14 Electrostatic properties of (quercetin) side views of the dipole and the Mullikan charge populations are displayed on the left while the middle and right panels show the isosurface representation of electrostatic potential (the electron rich region is red and the electron poor region is blue).

CONCLUSION

It was found that quercetin behaves as a mixed type inhibitor, retarding both anodic metal dissolution and cathodic hydrogen evolution reactions. Thus, quercetin acts as a temperature-independent inhibitor. The inhibition efficiency of the quercetin increases with the increase of inhibitor concentration to reach 98.2 % at $2 \cdot 10^{-6} \text{M}$. Data obtained from EIS studies were analyzed to determinate the model inhibition process through appropriate equivalent circuit models. The adsorption process of the studied inhibitor obeys the Langmuir adsorption isotherm and the adsorption behavior of quercetin includes both physisorption and chemisorption. Quantum chemical calculations showed a good correlation between quantum chemical parameters for the investigated compound and its inhibition efficiency for the corrosion process in agreement with experimental results.

Acknowledgment

The authors would like to thank the Palestenian Ministry of Higher Education. Also, we would like to extend our thanks to Palestine Water Authority (PWA) and MEDRIC for their support. The support given through an "INCRECYT" research contract to M. Zougagh is also acknowledged.

REFERENCES

- [1] A Espinoza-Vázquez, GE Negrón-Silva, D Angeles-Beltrán, H Herrera-Hernández, M R Romo, M Palomar-Pardavé, *Int. J. Electrochem. Sci.*, **2014**, 9, 493.
- [2] B Dog̃ru Mert, A O Yuce, G Kardas, B Yazıcı, *Corros. Sci.*, **2014**, 85, 287.
- [3] VV. Torres, VA. Rayol, M Magalhães, GM Viana, LCS Aguiar, SP Machado, H Orofino, E D'Elia, *Corros. Sci.*, **2014**, 79, 108.
- [4] A Yuce , B Mert, G Kardas, B Yazıcı, *Corros. Sci.*, **2014**, 83, 310.
- [5] S. Hari Kumar, S. Karthikeyan, *J. Mater. Environ. Sci.* **2013** 4,675.
- [6] A Abdel Nazeer, HM El-Abbasy, AS Fouda, *Res. Chem. Intermed.* **2013**, 39, 921.
- [7] L Afia, R Salghi, O Benali, S Jodeh, I Warad, E Ebenso , B Hammouti, *Port. Electrochim. Acta*, **2015**, 33(3), 137.
- [8] L Afia, O Benali, R Salghi, E E Ebenso, S Jodeh, M Zougagh, B Hammouti, *Int. J. Electrochem. Sci.*, **2014**, 9, 8392.
- [9] O Benali, H Benmehdi, O Hasnaoui, C Selles, R Salghi, *J. Mater. Environ. Sci.*, **2013**,4, 127.
- [10] MT Saeed, *Anti-Corros. Met. Mater.* **2004**, 51, 389.
- [11] P.R. Roberge, *Handbook of Corrosion Engineering*, McGraw-Hill, NY, **2000**.
- [12] V. Sastri, *Corrosion Inhibitors: Principles and Applications*, John Wiley & Sons, Inc., Hoboken, New Jersey, **2011**.
- [13] J. Cheng, X. Chen, S.Zhao, Y. Zhang, *Food.Chem*, **2015**, 168, 90.
- [14] M Plaza, T Pozzo, J Liu, K Z Gulshan Ara, C Turner, E J N Karlsson, *Agr. Food.Chem*, **2014**, 62(15) 3321.
- [15] N Terahara, *Nat Prod Commun*, **2015**, 10(3), 521.

-
- [16] MJ Frisch , GW Trucks, HB Schlegel , GE Scuseria, MA Robb, JRCheeseman JR Jr.Gaussian03, revision E.01.Walling ford, CT: Gaussian Inc. (2007).
- [17] R Solmaz, *Corros. Sci.* **2010**, 52, 3321.
- [18] XH Li, SD Deng, H Fu, *Corros. Sci.* **2009**, 51, 1344.
- [19] S Kertit, B Hammouti, *Appl. Surf. Sci.* **1996**, 93, 59.
- [20] F Mansfeld, MW Kending, S Tsai, *Corros.* **1982**, 37, 301 .
- [21] F Bentiss, M Lebrini, M Lagrenée, *Corros. Sci.* **2005**, 47, 2915.
- [22] M Benabdellah, A Aouniti, A Dafali, B Hammouti, M Benkaddour, A Yahyi, A Ettouhami, *Appl. Surf. Sci.* **2006**, 13 252
- [23] M Benabdellah, A Yahyi, A Dafali, A Aouniti, B Hammouti, A Ettouhami, *Arabian. J. Chem* ,**2011**, 4, 243.
- [24] H Shih, H Mansfeld, *Corros. Sci.* **1989**, 29, 1235.
- [25] S Martinez, M Metikos-Hukovic, *J. Appl. Electrochem*, **2003**,33 1137.
- [26] A Kosari, M Momeni, R Parvizi, M Zakeri, MH Moayed, A Davoodi, H Eshghi, *Corros. Sci.* **2011**, 53, 3058.
- [27] FB Growcock, RI Jasinski, *J. Electrochem. Soc.* **1989**, 136, 2310.
- [28] M Behpour, SM Ghoreishi, N Soltani, M Salavati-Niasari, *Corros. Sci.* **2009**, 51, 1073.
- [29] LM Vrac̃ar, DM Draz̃ic̃ , *Corros. Sci.* **2002**, 44, 1669.
- [30] SS Abd-El-Rehim, SAM Refaey, F Taha, MB Saleh, RA Ahmed, *J. Appl. Electrochem.* **2001**, 31, 429
- [31] MM Kabanda, LC Murulana, M Ozcan, F Karadag, I Dehri, IB Obot, EE Ebenso, *Int. J. Electrochem. Sci.* **2012**,7, 5035.
- [32] MA Quraishi and R Sardar, *J.Appl.Electrochem.*, **2003**, 33(12), 1163-1168.